DEVELOPMENT OF AN ELECTRICAL STIMULATION DEVICE FOR OSSEOINTEGRATED AMPUTEES

A Novel Approach for Expediting Skeletal Attachment and Rehabilitation

Brad Isaacson[1,2], Jeroen Stinstra[3], Rob MacLeod[2,3] and Roy Bloebaum[1,2,4]
[1]*Department of Veteran Affairs, Salt Lake City, UT, U.S.A.*
[2]*Department of Bioengineering, Univerisity of Utah, Salt Lake City, UT, U.S.A.*
[3]*Scientific Computing Institute, University of Utah, Salt Lake City, UT, U.S.A.*
[4]*Department of Orthopedics, University of Utah, Salt Lake City, UT, U.S.A.*

Keywords: Osseointegration, Electrical stimulation, Osteogenesis, Percutaneous, Amputation.

Abstract: The projected number of American amputees is expected to rise to 3.6 million by 2050. Many of these individuals depend on artificial limbs to perform routine activities, but prosthetic suspensions using traditional socket technology can prove to be cumbersome and uncomfortable for a person with limb loss. Moreover, for those with high proximal amputations, limited residual limb length may prevent exoprosthesis attachment all together. Osseointegration technology is a novel operative procedure that allows integration between host tissue and an orthopaedic implant and has been shown to improve clinical outcomes by allowing direct transfer of loads to a bone-implant interface. However, the associated surgical procedures require long rehabilitation programs that may be reduced through expedited skeletal attachment via electrical stimulation. To determine optimal electrode size and placement, we have developed a system for computational modeling of the electric fields that arise during electrical stimulation of residual limbs. Three patients with retrospective CT scans were selected and three dimensional reconstructions were created using customized software (Seg3D and SCIRun). These software packages supported the development of patient specific models and allowed for interactive manipulation of electrode position and size; all variables that could affect the electric fields around a percutaneous osseointegrated implant. Preliminary results of the electric fields at the implant interface support the need for patient specific modeling in order to achieve the homogenous electric field distribution required to induce osteoblast migration and enhance skeletal fixation.

1 INTRODUCTION

Osseointegration implant technology is a novel surgical procedure that provides direct skeletal attachment between an implant and host tissue and can significantly increase the quality of life for amputees (Albrektsson & Albrektsson, 1987; Branemark, 1983). However, one challenge with using natural biological fixation is attaining a strong skeletal interlock at the implant interface, a prerequisite for long-term implant function (Albrektsson, Branemark, Hansson, & Lindstrom, 1981). Therefore, we propose a means to accelerate osteogenesis through external electrical stimulation and present a simulation approach for which to develop such a system.

Veterans with combat related injuries form an especially relevant population that requires the development of new tools to enhance the success of osseointegration, due to their limited residual limbs caused by explosive devices. Improvements in medical care and evacuation strategies have led to an increase in survival rates, resulting in an elevated number of veterans with amputations that require follow-up care and extensive rehabilitation. The relative youth and otherwise good health of these amputees make them an ideal population for aggressive rehabilitation but also reveal the limitations of current technologies of prosthetic attachment (Hagberg & Branemark, 2001). Physical limitations with warrior amputees using sockets include heat/sweating in the prosthetic socket, skin irritation and inability to walk on challenging terrain (Hagberg & Branemark, 2001). In addition, a significant number of returning service men and

Isaacson B., Stinstra J., MacLeod R. and Bloebaum R. (2009).
DEVELOPMENT OF AN ELECTRICAL STIMULATION DEVICE FOR OSSEOINTEGRATED AMPUTEES - A Novel Approach for Expediting Skeletal Attachment and Rehabilitation.
In *Proceedings of the International Conference on Biomedical Electronics and Devices*, pages 178-185
DOI: 10.5220/0001511501780185

women have short residual limbs for which socket technology is not suitable.

Utilizing metallic implants as a means of biological fixation has been the objective of orthopedic surgeons over the past two centuries (Williams, 1982). However, controlling osteogenesis at the implant interface, which is essential for providing strong skeletal fixation, remains challenging. Regulated electrical stimulation has proven effective in fracture healing and non-traumatized bone models (Brighton, 1981; Friedenberg, Zemsky, Pollis, & Brighton, 1974), but has not been investigated in a percutaneous osseointegrated implant system. One advantage of this patient population is that an orthopedic implant protrudes from the residual limb functioning as an exoprosthesis attachment and a potential cathode for an external electrical stimulation device.

By understanding the method of current injection with varying electrode size and placements, an electric field on the magnitude of 1-10 V/cm may be established at the implant interface, capable of inducing osteoblast migration and improving skeletal attachment (Ferrier, Ross, Kanehisa, & Aubin, 1986). An electric field of this degree may increase the quantity and quality of bone at the implant interface, and thus would improve the prospects for accelerated rehabilitation and skeletal fixation for an amputee. Figure 1 contains a schematic of a stimulation apparatus that we envision.

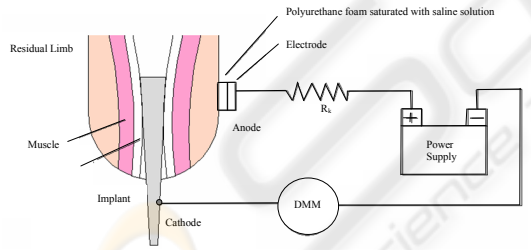

Figure 1: Representative model of the electrical stimulation device proposed for amputees with a percutaneous osseointegrated implant.

The initial approach to develop an electrical stimulation osseointegration system is to simulate electric field strength on a patient specific basis using a computational model. Because variations in electrode size and placement could inhibit or expedite bone growth, the modeling approach includes both the electrode placement for stimulation at the skin as well as patient specific anatomy to determine an accurate estimate of the underlying electrical simulation fields.

The objective of our research is to develop an alternative means of prosthetic suspension superior to the traditional socket method for patients with amputations. This goal is strongly motivated by the growing rate of amputations occurring annually from vascular occlusive diseases, diabetes, and traumatic injury. While an amputation can be a life saving surgical procedure, many interpret the operation as a significant loss, which alters "the perception of an individual of his or her degree of physical, psychological and social well-being and the effects that illness and treatment have on daily life" (Hagberg & Branemark, 2001). We demonstrate here the feasibility of a computational approach to developing such a system.

2 METHODS

2.1 Overview

In order to simulate the electric field that is present at the bone-implant interface, three patient specific models were created. A volume conductor model was developed to compute realistic electric fields from computer tomography (CT) scans of the limbs of these patients by assigning tissue conductivities during segmentation. Using this model and assuming that the electrical field can be calculated using a quasi-static approach, the electrical potential was computed by solving Laplace's equation for each tissue type.

$$\nabla \cdot \sigma \nabla \varphi = 0 \tag{1}$$

In this model the boundary conditions were formed by the electrodes that injected currents and the guideline that current remained within the body. Since the electrodes and the implant had a much larger conductivity than the surrounding tissues, it was assumed that the implant (cathode) was at a constant potential, likewise the surface electrodes were modeled with a constant potential difference from the percutaneous implant.

Numerical simulation was used to compute the electric potential through the CT scans of the patient's residual limb. To evaluate the efficacy of electrode configuration and sizing, patient specific models were developed and the electrical potential around the implant interface was used to determine localized electric field strengths.

2.2 Image Acquisition

CT images were obtained retrospectively from the radiology department at the University of Utah in accordance with Institutional Review Board (IRB) approval. Femoral slice thicknesses ranged from 600 µm to 1 mm and of the 50 patients examined, 3 were selected based on predetermined demographics and absence of metallic implants, which cause image artifacts. Table 1 lists patient specifics.

Table 1: Patient Demographics.

Patient	Sex	Amputee	Age	Height [cm]	Weight [kg]
1	M	No	60	185.4	79.9
2	F	No	28	157.5	50.1
3	F	Yes	80	152.4	45.5

To determine the variability amongst patients, only one amputee was selected from the population (Patient 3). The remaining two models were generated from subjects in the general population who were made into "artificial amputees" from segmentation using computer software. To account for natural anatomical differences in patient limbs, wide variation in age (SD = 26.2), height (SD = 17.8) and weight (SD = 18.7) were selected.

Establishing accurate tissue differentiation was performed using the Seg3D (www.seg3d.org) software. The tissue boundaries of the bone, bone marrow and adipose tissue were generated by thresholding the CT images interactively. The musculature was obtained by manually setting seed points inside the muscle tissue and using a confidence connected filter to find all the tissue connected to the seed points. Finally, the skin, which was impossible to discern reliably from the CT images, was generated by dilating the outermost tissue 2 millimeters based on average skin thickness to produce a layer of homogeneous thickness that surrounded the full model (Tortora & Nielsen, 2008). Segmentations were manually inspected, corrected to ensure accuracy and combined in a hierarchy into a single label map required for finite element analysis. An example of a segmentation, consisting of skin, adipose tissue, muscle, bone and bone marrow is depicted in Figure 2.

2.3 Electrode Placement & Design

Since there are no preliminary results using such a system for a percutaneous osseointegrated implant, we selected four widely variable electrode configurations for testing. Small electrodes were designed with patient compliance in mind, since the device should not restrict ambulation or daily activity.

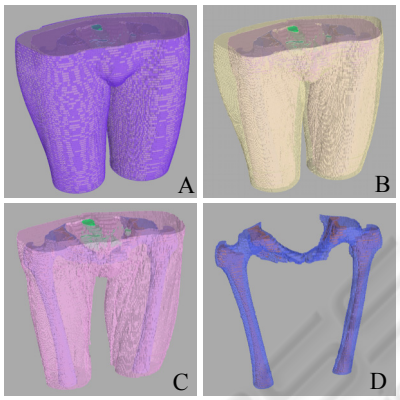

Figure 2: Hierarchical label maps constructed in Seg3D for Patient 2. The completed femoral mapping was composed of skin (A), adipose tissue (B), musculature (C), bone (D) and bone marrow (D).

The SCIRun (software.sci.utah.edu) software package was utilized for electrode design because it supports interactive electrode placement and simulation. The configurations selected consisted of a one patch electrode, two patch electrodes, one continuous band and two continuous bands (Figure 3). External electrode bands were applied on the residual limb of the patient and were 1.6 cm in thickness. Electrode patches were placed as a strip covering approximately half the diameter of the leg and were 3 cm in thickness. Lastly, the percutaneous implants were set to match the size of the cavity of the bone marrow to represent proper implant fit and fill, since gaps in excess of 50 µm may lead to fibrous encapsulation without bone ingrowth (Bloebaum, Bachus, Momberger, & Hofmann, 1994; Hofmann, Bachus, & Bloebaum, 1993).

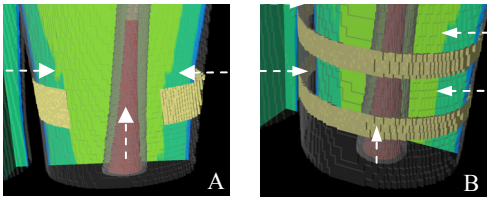

Figure 3: Electrode configurations modeled to determine optimal performance for amputees. The electrode configuration is shown from patient 2. A two patch setup was changed to a one patch setup by removing the medial electrode (A). A double band electrode was altered to a single band configuration by removing one band and centering it amongst the implant area (B). Electrode size and position are illustrated with arrows.

2.4 Finite Element Analysis

In order to predict electric fields from exogenous voltage potentials, label maps and electrodes were modeled using a hexahedral mesh that consisted of approximately 1.7 million elements. The elements were treated as piecewise homogenous, ohmic and isotropic, and were assigned conductivities using previously published values and estimations by the investigators (Chiu & Stuchly, 2005; Gabriel, Lau, & Gabriel, 1996; Stinstra et al., 2007) (Table 2). Because tissue behaves inherently electrolytic, treating the models with DC conductivities was considered to be an important factor (Grimnes & Martinsen 2008).

Electrodes were incorporated in the finite element meshing and assigned a constant potential difference of 9 volts between the skin electrode and osseointegrated implant, a selection based on expected tissue resistivity. Using an iterative solver, the potentials in the finite element models were computed for the three patients and four electrode configurations.

Table 2: Conductivity values assigned to segmentations.

Tissue Type	Conductivities [S/m]
Skin	0.26
Muscle	0.25
Adipose	0.09
Organ	0.22
Cortical Bone	0.02
Bone Marrow	0.07

2.5 Data Analysis

In order for an electrode configuration to be deemed acceptable, a uniform homogenous field around the implant interface was required for bone growth. Therefore, histograms were computed for about 6000 elements in the immediate area encompassing the bone implant interface. The results were analyzed using maps of electric field strength that show the variability of the electric field within the leg.

3 RESULTS

Interactive placement of electrodes allowed for various computational simulations. Figure 4 illustrates one example of the differences between patients. The figure depicts cross sections for three different patients, where the color scale indicates the strength of the local field. The corresponding histogram (right) represents the electric field strength of the 6000 elements surrounding the implant site and shows the homogeneity of the field. The histograms showed a broad variation among patients, some producing normal Gaussian distributions and others with broad or skewed peaks and thus a higher than random level of homogeneity. The complete set of histograms used for analysis is listed subsequently in Figure 5.

4 DISCUSSION

The necessity for patient specific models with a percutaneous electrical stimulation device was confirmed in the study. The distribution of electrical potentials at the implant-bone interface varied across subjects due to variations in anatomy and the presence of an amputation. While creating “artificial amputees” using a segmentation program was straightforward and permitted robust computation, histograms of electric field strength confirmed that electrical metrics changed dramatically when compared to a known amputee. While the shape of the histograms tended to be bell shaped, the position of the peaks were often skewed depending on the electrode configuration and patient. The results clearly showed that the 1 patch electrode generates the smallest electric field in the bone-implant interface, while the 2 band electrode configuration generated the highest field for the same applied potential, suggesting that proper electrode placement could improve efficiency.

Due to the limited quantity of patients in the study, a strong correlation was not established relating patient demographics with voltage potentials. However, the highest voltage gradients mapped during simulations were consistently from subject 2, a patient who was in the best physical condition. The increased electrical field was likely caused by the reduction in the diameter and thickness of adipose tissue in the subject’s residual limb, since adipose tissue would raise resistivity and impede current flow.

While an optimal electrical configuration may not have been established for the patient population collectively, two bands appeared to produce the most homogenous electrical field distributions between 1-10 V/cm. Minor adjustments would be required if the device were used clinically to account for the varying anatomy of patients, spatial location of topical electrodes and may be confirmed with CT files and computational modeling.

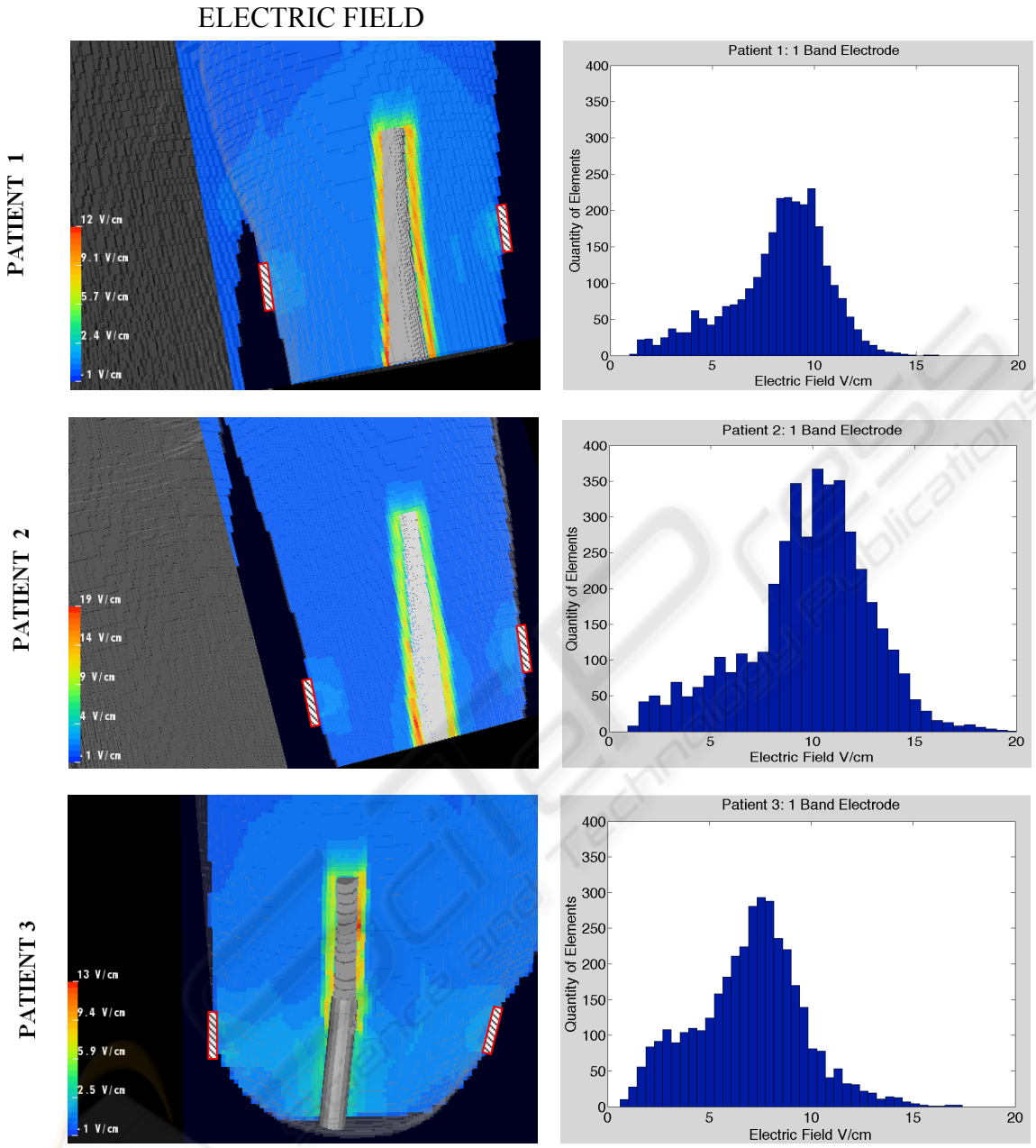

Figure 4: Sample distributions of the electric field strength surrounding the implant. The color map reflects the strength of the electric field in a cross section through the lower part of the limb. External electrode placements were illustrated as rectangular objects on the outside of the residual limb. The results were for an 18 centimeter percutaneous implant that was interactively inserted into the medullary canal of adult patients. The histograms on the right represent the distribution of the electric field strength in the volume next to the implant.

While the initial target of the exogenous electrical stimulation system utilizes an orthopedic implant as a functional cathode, it may also reduce the potential for superficial and deep infections by preventing additional surgical procedures to remove implanted devices as seen with older fracture healing models (Lavine & Grodzinsky, 1987). However, the success of the system is dependent on numerous factors including hydration levels, quantity of soft tissue and the material type selected for the orthopedic implant. In order for this novel technology to be beneficial, a balance must be

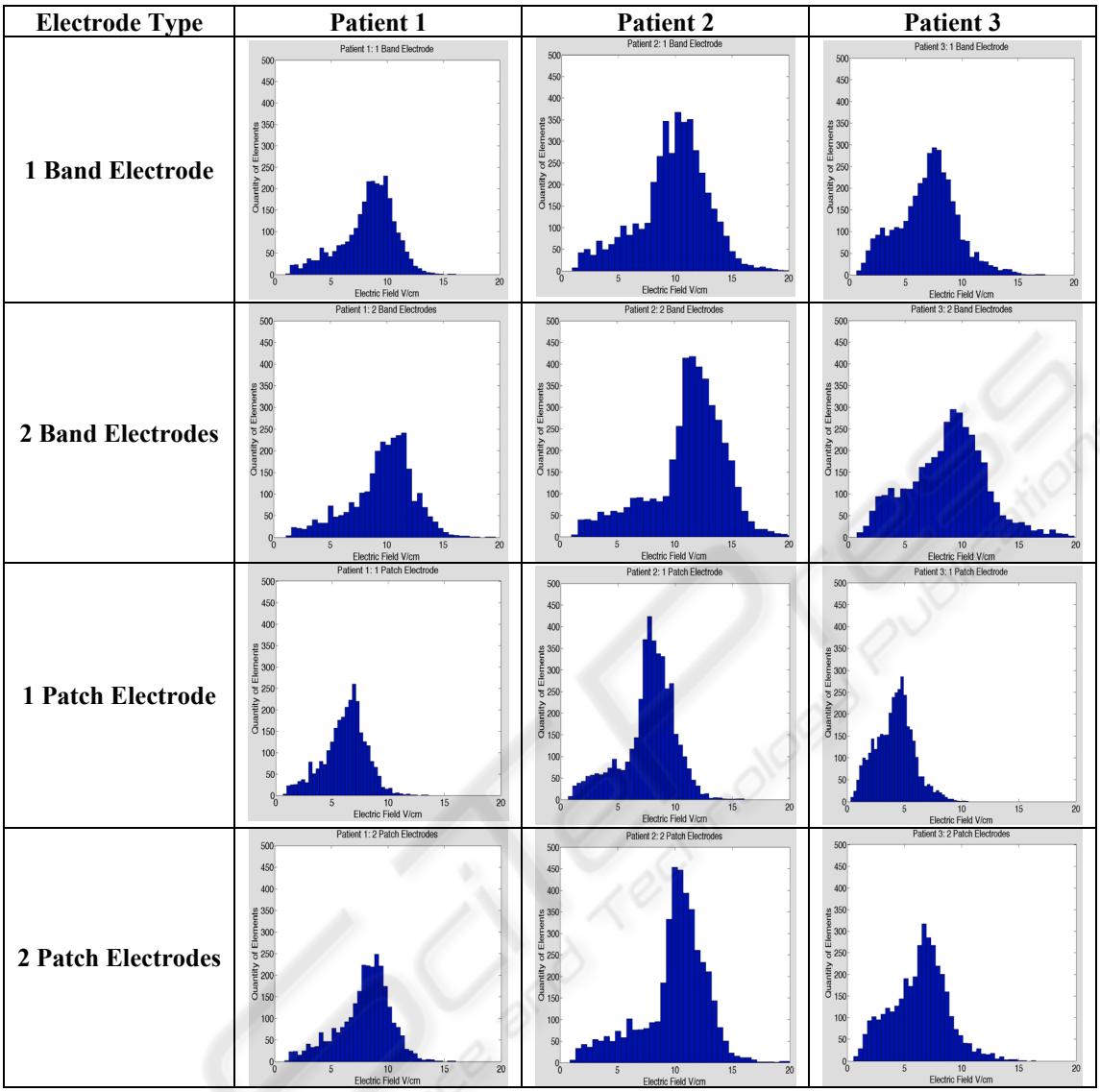

Figure 5: Comparison between patients and electrode configurations. The results confirm the requirement for individual patient modeling. Distributions of electric fields were not homogenous in each case and would require manipulation of the applied voltage potential to attain uniform bone ingrowth.

attained between obtaining a desired electric field and the host tissue reaction which may occur with varying implanted metals. Titanium alloy was selected as the cathode in this model ($3x10^6$ S/m) since it is regarded as the one of the most biocompatible material type for total joint replacements and has low thermal conductivity to protect tissue necrosis from heat generation (Agins et al., 1988; Beder & Eade, 1956; Emneus & Gudmundsson, 1967). However, if clinicians and engineers require an altered rate of electron propagation, the material can be exchanged (Grimnes & Martinsen, 2008) or porosity altered but careful attention should be paid to ensure the material does not illicit a foreign body response.

Utilizing electrical stimulation for older amputees is a critical aspect which must be explored as well. Bone mass is maximum a decade after skeletal growth ceases but decreases significantly by the eighth and ninth decade (Buckwalter, Glimcher, Cooper, & Recker, 1995). As long bones change confirmation with age, the endosteal diameter tends to increase more rapidly than the periosteal diameter which could lead to implant loosening (Lane & Vigorita, 1983). This problem coupled with the reduction of strain on bones by weaker muscles may

contribute to debilitating diseases such as osteoporosis and osteopenia (Lane & Vigorita, 1983) and require additional treatment options. However, controlled electrical stimulation and mechanical loading may act as a synergistic catalyst of bone ingrowth (Spadaro, 1997) and maintain host bone bed integrity with elderly patients using an osseointegrated electrical implant system.

Establishing tools for enhancing skeletal attachment may assist with reducing the length of rehabilitation required for an osseointegrated procedure. Current programs require 2 to 24 months of rehabilitation (Branemark, Branemark, Rydevik, & Myers, 2001), a lengthy time period to ensure uniform ingrowth. Because of the slow biological process of skeletal attachment, loading at the implant interface would be restricted for several months after the operative procedure (Hofmann, Bloebaum, & Bachus, 1997). However, using an electrical stimulation system may enhance ingrowth and allow patients to return to earlier ambulation.

4.1 Limitation

Since the conductivity of a titanium implant significantly exceeded that of cortical bone, the current densities at the implant interface should be modeled to ensure localized tissue heating does not occur, which may lead to patient discomfort or potential tissue necrosis. Computational modeling of current density fields are attainable with the given software package and will be utilized in future work. Additional efforts with be paid to altering the porosity of the titanium implant and determining the effect on the predicted electric fields since porosity and conductivity are inversely related and may affect the model as well (Ke et al., 2007).

5 CONCLUSIONS

The simulations developed for the proposed biomedical device may have the capabilities of expediting skeletal attachment by increasing osteoblast migration. Computation modeling has effectively shown that 1-10 V/cm electric fields may be generated using the implant as a functional cathode and topically applied anode band and patches. Implementing computational models may be the first step to resolving the classic problem with electrical stimulation which is the inability to define current pathways in the human body (Chakkalakal & Johnson, 1981; Noda & Sato, 1985).

Patient specific modeling was effective for attaining values that may be osteogenic at the implant site, but wide variations in electric field distributions shown in histograms reaffirm the need to evaluate each case specifically. However, in order to determine the accuracy of finite element analysis, the quantity of subjects will be increased in the future work to determine if an electrode configuration could be optimized for patients with percutaneous osseointegrated implants. Additional model validation of electrically enhanced osseointegration will be assessed using a small *in vivo* animal model based on computational evidence in future work.

ACKNOWLEDGEMENTS

This material is based upon research supported by the Office of Research and Development, Rehabilitation R&D Service, DVA SLC Health Care System, Salt Lake City, Utah; the Albert & Margaret Hofmann Chair and the Department of Orthopaedics, University of Utah School of Medicine, Salt Lake City, Utah. Additional technical support for the simulations was provided by the Center for Integrative Biomedical Computing of Scientific Computing and Imaging Institute and *was made possible in part by software from the NIH/NCRR Center for Integrative Biomedical Computing, P41-RR12553-07*.

REFERENCES

Agins, H. J., Alcock, N. W., Bansal, M., Salvati, E. A., Wilson, P. D., Pellicei, P. M., et al. (1988). Metallic wear in failed titanium-alloy total hip replacements. *J. Bone Joint Surg. [Am.], 70-A*(3), 347-356.

Albrektsson, T., Branemark, I.-I., Hansson, H.-A., & Lindstrom, J. (1981). Osseointegrated titanium implants. *Acta Orthop Scand, 52*, 155-170.

Albrektsson, T., & Albrektsson, B. (1987). Osseointegration of bone implants. A review of an alternative mode of fixation. *Acta Orthop Scand, 58*(5), 567-577.

Beder, O. E., & Eade, G. (1956). An investigation of tissue tolerance to titanium metal implants in dogs. *Surgery, 39*(3), 470-473.

Bloebaum, R. D., Bachus, K. N., Momberger, N. G., & Hofmann, A. A. (1994). Mineral apposition rates of human cancellous bone at the interface of porous coated implants. *J Biomed Mater Res, 28*(5), 537-544.

Branemark, P. I. (1983). Osseointegration and its experimental background. *J Prosthet Dent, 50*(3), 399-410.

Branemark, R., Branemark, P. I., Rydevik, B., & Myers, R. R. (2001). Osseointegration in skeletal reconstruction and rehabilitation: a review. *J Rehabil Res Dev, 38*(2), 175-181.

Brighton, C. T. (1981). The treatment of non-unions with electricity. *J Bone Joint Surg Am, 63*(5), 847-851.

Buckwalter, J. A., Glimcher, M. J., Cooper, R. R., & Recker, R. (1995). Bone biology. *J Bone Joint Surg Am, 77*(2), 1276-1289.

Chakkalakal, D. A., & Johnson, M. W. (1981). Electrical properties of compact bone. *Clin Orthop Relat Res*(161), 133-145.

Chiu, R. S., & Stuchly, M. A. (2005). Electric fields in bone marrow substructures at power-line frequencies. *IEEE Trans Biomed Eng, 52*(6), 1103-1109.

Emneus, H., & Gudmundsson, G. (1967). Final report on clinical testing of titanium. *Acta Orthop Scand*, 372-373.

Ferrier, J., Ross, S. M., Kanehisa, J., & Aubin, J. E. (1986). Osteoclasts and osteoblasts migrate in opposite directions in response to a constant electrical field. *J Cell Physiol, 129*(3), 283-288.

Friedenberg, Z. B., Zemsky, L. M., Pollis, R. P., & Brighton, C. T. (1974). The response of non-traumatized bone to direct current. *J Bone Joint Surg Am, 56*(5), 1023-1030.

Gabriel, S., Lau, R. W., & Gabriel, C. (1996). The dielectric properties of biological tissues: III. Parametric models for the dielectric spectrum of tissues. *Phys Med Biol, 41*(11), 2271-2293.

Grimnes, S. & Martinsen O. (2008). *Bioimpedance and Bioelectricity Basics*. Amersterdam: Academic Press.

Hagberg, K., & Branemark, R. (2001). Consequences of non-vascular trans-femoral amputation: a survey of quality of life, prosthetic use and problems. *Prosthet Orthot Int, 25*(3), 186-194.

Hofmann, A. A., Bachus, K. N., & Bloebaum, R. D. (1993). Comparative study of human cancellous bone remodeling to titanium and hydroxyapatite coated implants. *J. Arthroplasty, 8*(2), 157-166.

Hofmann, A. A., Bloebaum, R. D., & Bachus, K. N. (1997). Progression of human bone ingrowth into porous-coated implants. *Acta Orthop. Scand., 68*(2), 161-166.

Ke, Z., Cheng-Feng, L., & Zhen-Gang, Z. (2007). Measurement of Electrical Conductivity of Porous Titanium and Ti6Al4V Prepared by the Powder Metallurgy Method.. *Chin. Phys. Lett., 24*(1), 187-190.

Lane, J. M., & Vigorita, V. J. (1983). Osteoporosis. *J Bone Joint Surg Am, 65*(2), 274-278.

Lavine, L. S., & Grodzinsky, A. J. (1987). Electrical stimulation of repair of bone. *J Bone Joint Surg Am, 69*(4), 626-630.

Noda, M., & Sato, A. (1985). Appearance of osteoclasts and osteoblasts in electrically stimulated bones cultured on chorioallantoic membranes. *Clin Orthop Relat Res* (193), 288-298.

Spadaro, J. A. (1997). Mechanical and electrical interactions in bone remodeling. *Bioelectromagnetics, 18*(3), 193-202.

Stinstra, J. G., Jolley, M., Callahan, M., Weinstein, D., Cole, M., Brooks, D. H., et al. (2007). Evaluation of different meshing algorithms in the computation of defibrillation thresholds in children. *IEEE Engineering in Medicine and Biology Conference*.

Tortora, J. & Nielsen M. (2008). *Principles of Human Anatomy* (11th ed). United States: John Wiley & Sons.

Williams, D. F. (1982). Biocompatibility of Orthopedic Implants. Volume I. In D. F. Williams (Ed.), *CRC Series in Biocompatibility* (pp. 141-195). Liverpool: CRC Press, Inc.